A DNS Study of the Effects of Injection Timing on the Ignition of PRF/Air Mixture under Direct Dual Fuel Stratification (DDFS) Conditions

Minh Bau Luong[1], Ramanan Sankaran[2], Gwang Hyeon Yu[1], Suk Ho Chung[3], Chun Sang Yoo[1,*]

[1] School of Mechanical and Nuclear Engineering, Ulsan National Institute of Science and Technology, Ulsan 44919, Republic of Korea

[2] National Center for Computational Sciences, Oak Ridge National Laboratory, Oak Ridge, TN 37831, USA

[3] Clean Combustion Research Center, King Abdullah University of Science and Technology, Thuwal, Saudi Arabia

Abstract

The effects of injection timing on the direct dual fuel stratification (DDFS) combustion are investigated using 2-D direct numerical simulations with a 116-species reduced PRF mechanism. *iso*-Octane and *n*-heptane are chosen as two different fuels of low and high reactivity, respectively. A pseudo *iso*-octane model is developed to simulate the multiple injections. It is found that DDFS combustion is highly sensitive to the injection timing. If *iso*-octane is delivered into the undergoing-reacting charge, the overall DDFS combustion after the late injection occurs primarily through auto-ignition and its burning rate is mainly governed by diffusion-limited injection.

1. Introduction

Reactivity controlled compression ignition (RCCI) combustion has demonstrated superior controllability of the combustion process without sacrificing the benefits of conventional HCCI combustion such as high thermal efficiency, improved fuel consumption, and ultra-low emissions [1-2]. Typically, RCCI uses two fuels with different autoignition characteristics. Low-reactivity fuel is supplied through port injection to ensure it well mixed with the oxidizer. One or more direct injections of high-reactivity fuel are followed to create spatial inhomogeneities in reactivity and equivalence ratio. By adjusting the mass ratio of two fuels and the timing/duration of direct injections of high-reactivity fuel, RCCI can provide a fast-response control of the ignition timing and combustion duration.
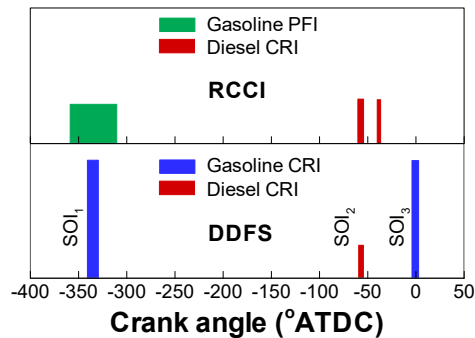

Figure 1. Illustration of RCCI and DDFS combustion concepts reproduced from [3].

However, the high-load operating range of RCCI combustion is limited by the reactivity of premixed fuel. As load increases, the combustion phasing is prone to advance, which can be counteracted by reducing the amount of high-reactivity fuel. This amount tends to decrease to zero as load is high enough. At this point, there are no longer any direct control mechanisms of the combustion phasing and combustion process. Moreover, the port-injected low-reactivity fuel is fully premixed and thus nearly homogeneous, consequently, its combustion occurs volumetrically similar to HCCI combustion. This results in excessively high rates of the pressure rise, and in turn limiting load.

One remedy for extending the high-load limit of RCCI is to stratify both fuels by injecting gasoline and diesel directly into the cylinder. This method allows more flexible controllability over the in-cylinder reactivity distribution of two fuels. By using a multiple-injections scheme as conceptually shown in Fig. 1, Wissink and Reitz demonstrated that compared to RCCI, direct dual fuel stratification (DDFS) is more beneficial for distributing HRR and reducing PRR at high load conditions [3-5]. In DDFS, the start of the heat release is controlled by the diesel injection, while the peak and duration of the heat release rate are governed by a near-TDC gasoline injection. In particular, similar to RCCI, DDFS uses an early injection of gasoline to create a premixed background charge, followed by a direct injection of diesel to generate some degrees of reactivity and equivalence ratio stratification. These two injections are designed to control the start of the main combustion prior to TDC. Inspired by PPC, DDFS utilizes a high-pressure direct injection of gasoline right before TDC. As such, DDFS provides a capability of independently controlling combustion timing and combustion duration by combining reactivity stratification with a diffusion-limited gasoline injection. However, the effect of the timing of the late gasoline injection on the combustion process of both fuel stratification is not well-understood.

In previous DNS studies, the initial fields of HCCI combustion were typically configured after the time assuming that all the multiple injections have been finished to save computational time and cost [6-14]. For multiple injection strategies, the previous approach is, however, not capable of reproducing the timing and duration of a late direct injection, especially for cases in which the remaining fuel may be injected into an undergoing reacting charge as in [3-5].

Therefore, the objective of the present study is twofold: (i) to develop a pseudo-*iso*-octane model to mimic the timing and duration of a late direct injection, and (ii) to investigate the effect of the late-direct-injection timing on the combustion process of a primary reference fuel (PRF)/air mixture with stratification in both fuels under DDFS conditions using direct numerical simulations (DNSs).

2. Numerical method and initial conditions
2.1 Motor pressure

The effects of the compression heating and expansion cooling by a piston motion are taken into account by adding/removing appropriate mass source terms in the governing equations [14] instead of moving the meshes or varying the volume of the computational domain. The additional mass source terms are adjusted to ensure uniform thermodynamic pressure in the computational domain. Figure 2 shows the modeled motored-pressure trace that perfectly matches the experimental one without any noticeable discrepancies in the time duration of interest considered in the present study. The relevant engine parameters are taken from [3] with the compression ratio, intake pressure, and engine speed of 14.88, 1.84 atm, and 1300 rpm, respectively.
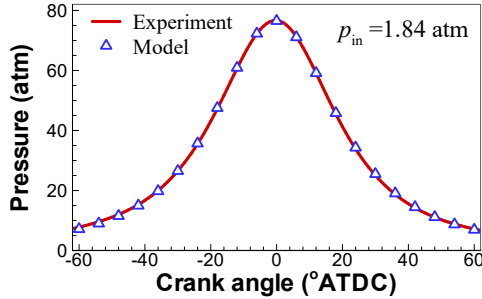

Figure 2. Experimental and modeled motored-pressure traces as a function of crank angle. Experimental motored-pressure trace taken from experiment by Wissink et al. [3] operating at 1300 RPM under a high-load condition of p_{in} of 1.84 atm

2.2 Preudo-*iso*-octane model

A 116-species reduced mechanism of primary reference fuel (PRF) [8] is adopted. PRF is a mixture of *n*-heptane and *iso*-octane, which have been widely used as realistic surrogates for high- and low-reactivity fuels, diesel and gasoline, respectively.

Here, we develop the pseudo-*iso*-octane PC_8H_{18} model to simulate the effects of the late injection of gasoline with a two-step process. As part of the initial condition, a stratified *iso*-octane composition is added to the mixture field by using a pseudo-*iso*-octane molecule. The chemical species, PC_8H_{18}, that forms a stratified mixture field is non-reactive during the initial phases of the simulation. Once the simulation has advanced close to TDC, the PC_8H_{18} species is converted to the reactive *iso*-octane species. This introduces reactive *iso*-octane in the system at

the appropriate juncture when gasoline injection was needed. The consumption of PC_8H_{18} and its conversion to reactive octane occurs through a source term, which resembles a Gaussian function in time. The form of the Gaussian conversion function is chosen to achieve the desired timing and duration, t_{inj} and t_{dur}, of gasoline injection. This conversion step allows the effects of gasoline injection during active combustion to be simulated without numerical instability issues. While all of the thermochemical and transport properties of the PC_8H_{18} are chosen to identically match the properties of octane, the enthalpy of formation of PC_8H_{18} is chosen to be lower than that of octane. This difference in enthalpy of formation causes a drop in temperature, thereby allowing the simulations to also account for the temperature drop due to the latent heat of evaporation of direct gasoline fuel injection.

In summary, the basic idea behind the PC_8H_{18} model is that at beginning, PC_8H_{18} is initialized with other fuels (*n*-heptane + *iso*-octane), and acts as an inert gas. At a specific time, so-called t_{inj}, PC_8H_{18} is gradually converted to real *iso*-octane for a given time duration of t_{dur}, and become as a fuel to participate in the combustion process. The process of converting PC_8H_{18} to octane is representative of a late direct injection of gasoline. For illustration, Fig. 3 shows that PC_8H_{18} starts to be converted to octane via the Gaussian function at t_{inj} of -25°CA ATDC, and the effective injection time duration, t_{dur} (conversion time of PC_8H_{18} to octane) is approximately 0.8 ms. Note that the injection duration, t_{dur} of 0.8 ms, is chosen as in [3] for all the cases in the present study.
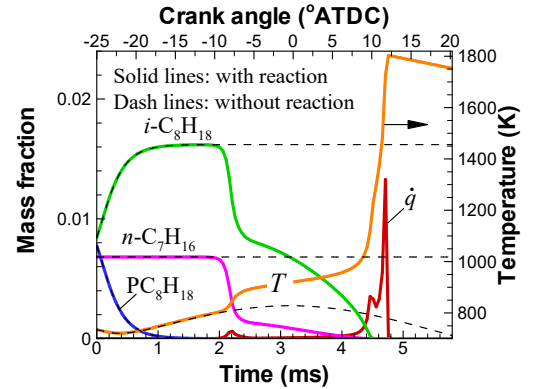

Figure 3. Temporal evolutions of the mass fraction of octane, PC_8H_{18}, and heptane, temperature, and heat release rate for 0-D ignition of Case 3 with and without combustion. The initial pressure, temperature, and t_{inj} are 35 atm, 735 K, and -25°CA ATDC, respectively. The effective injection duration, t_{dur}, is approximately 0.8 ms.

2.3 Initial conditions

S3D solver was used to solve a set of the Navier–Stokes equations for a chemically reacting fuel/air mixture. A 2-D domain of 3.2×3.2 mm^2 discretized with a grid resolution of 2.5 μm is used.

Case	Type	t_{inj} ms (°CA)	PRF_0	ϕ_0
1	BL	-	55	0.41
2	RCCI	-	70	0.60
3	DDFS	0.0 (-25.0)	70	0.60
4	DDFS	1.0 (-17.2)	70	0.60
5	DDFS	2.5 (-5.5)	70	0.60
6	DDFS	3.0 (-1.6)	70	0.60
7	DDFS	3.5 (2.3)	70	0.60

Table 1 Physical parameters of all seven cases.

All seven DNS Cases listed in Table 1 start at -25 °CA ATDC with the initial mean pressure, temperature, and equivalence ratio of 35atm, 735 K, and 0.6respectively. The mean fuel is PRF70 (70% *iso*-octane + 30% *n*-heptane by volume) for Cases 2−7. A dilution level of 40% mass fraction of EGR is added for all cases. Five DDFS cases (Cases 3-7) are performed by varying the injection timing of the late *iso*-octane direct injection, t_{inj} ranging from -25 to 2.3 °CA ATDC.

For DDFS cases, both PC_8H_{18} and $n\text{-}C_7H_{16}$ are initialized such that they are inhomogeneously superimposed onto a uniform $iso\text{-}C_8H_{18}$/(air + EGR) field. Specifically, both $n\text{-}C7H_{16}$ and PC_8H_{18} fields are initialized by $x = x_0 + x'$, where x denotes mole of either heptane or PC_8H_{18}, and x_0 of 0.324, and x' of 0.1 represent the mean value and variance, respectively. At a given time, t_{inj}, during the simulation, PC_8H_{18} is gradually converted into octane to account for the late injection process of octane. Different with Cases 3−7, for Case 1, PC_8H_{18} is not converted to $iso\text{-}C_8H_{18}$ such that the actual ϕ_0 and PRF_0 for Case 1 are 0.41 and PRF55, respectively.
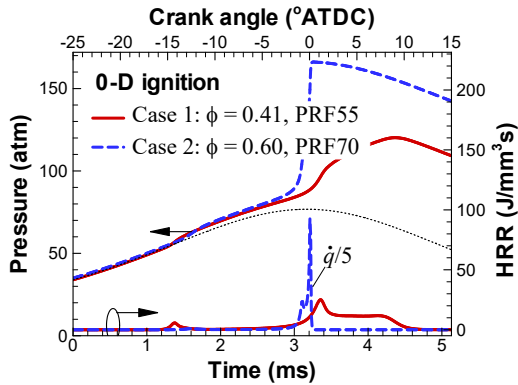

Figure 4. Temporal evolutions of the pressure and heat release rate for 0-D ignition of Cases 1 & 2 with. the initial pressure and temperature of 35 atm and 735 K, respectively. The dotted line is the modeled motored-pressure trace.

Case 2 representative of RCCI combustion is simulated. Unlike DDFS with both $n\text{-}C_7H_{16}$ and $iso\text{-}C_8H_{18}$ fluctuation (Cases 3−7), only $n\text{-}C_7H_{16}$ concentration fluctuation is generated for RCCI. $n\text{-}C_7H_{16}$ field is initialized by $x = x_0 + x'$, superimposed

onto a uniform octane/(air + EGR) field. Thanks to inhomogeneities in $n\text{-}C_7H_{16}$ concentration, stratification in reactivity (PRF) and equivalence ratio are attained. Figure 4 shows the temporal evolution of the pressure and HRR for 0-D ignition of Case 1 (PRF55, $\phi_0 = 0.41$), and Case 2 (PRF70, $\phi_0 = 0.60$).

The initial turbulent flow and scalar fields are prescribed by Passot-Pouquet spectrum functions with the same characteristic length scale of 1.2 mm. Turbulence intensity, u' of 0.4 is deliberately selected to ensure the turbulence time scale, $\tau_t = l_e / u' = 3.0$ ms equal to the ignition delay time of 3.2 ms. For illustration, the initial equivalence ratio and PRF fields with their relations are shown in Fig. 5−6.
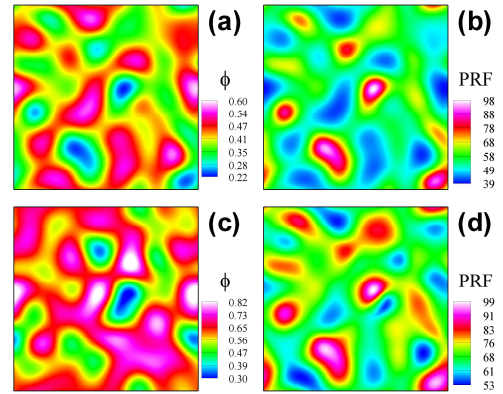

Figure 5. Initial equivalence ratio, and PRF fields (a-b) only $n\text{-}C_7H_{16}$ stratification and (c-d) both $n\text{-}C_7H_{16}$ and PC_8H_{18} stratification for DDFS cases 3-7
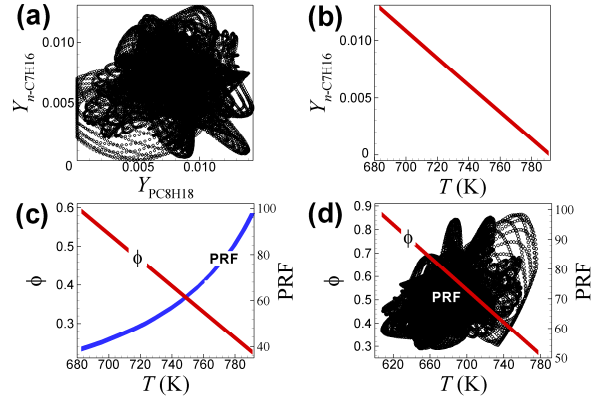
Figure 6. Scatter plots of (a) the mass fraction of $n\text{-}C_7H_{16}$ and PC_8H_{18} (uncorrelated), (b) $T\text{−}Y_{n\text{-}C7H16}$ (negatively-correlated), and (c) $T - \phi$ (negatively-correlated) and $T\text{−}PRF$ at the initial time, (d) $T - \phi$ and $T\text{−}PRF$ after injection.

3. Results and discussion

Figure 7 shows the temporal evolution of mean pressure and HRR for Cases 1−7. As readily seen in Fig. 7, Case 2 (RCCI combustion) exhibits the highest peak HRR and shortest combustion duration
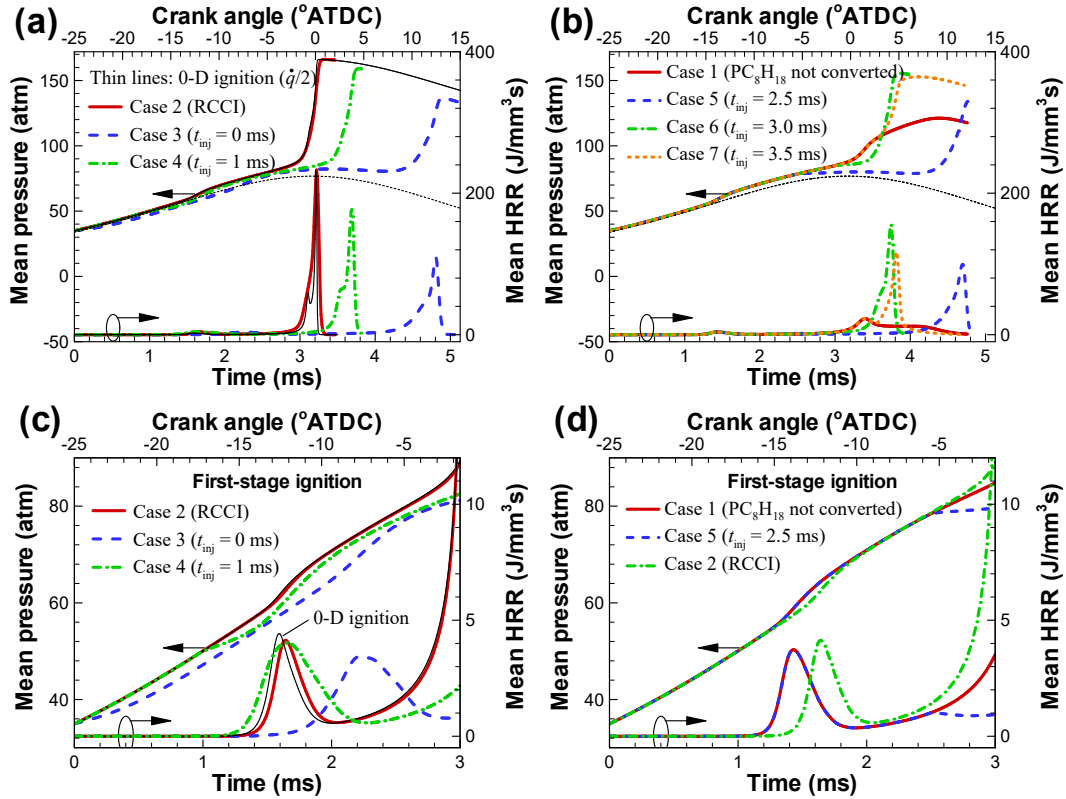
Figure 7. (a-b) Temporal evolutions of the mean pressure and mean HRR for Cases 1−7 (first row), and (c−d) their mean HRR during the first-stage ignition (second row). Note that the first-stage ignition of Cases 5−7 is identical to that of Case 1.

whereas Case 1 has the lowest peak HRR and longest combustion duration. It is primarily attributed to the difference in equivalence ratio. Case 1 with ϕ_0 of 0.41 is much leaner than Case 2 with ϕ_0 of 0.60. Despite the present of reactivity stratification, Case 2 still exhibits excessive HRR due to a very short combustion duration. It is because the ignition delay time decreases exponentially with increasing pressure during the compression stroke which in turn narrowing the differences in ignition delay time between adjacent fuel/air mixtures. The excessive HRR of Case 2 implies that under very high pressure of intake boosting, alternative methods such as DDFS are needed to alleviate such excessive HRR.

Unlike Case 2, Cases 3−7 (DDFS combustion) with a separate portion of the late direct-injected octane show a lower peak HRR by the slightly wider combustion duration. By adjusting the injection timing, t_{inj}, the overall combustion of DDFS tends to be delayed compared to that of RCCI. However, the combustion of Cases 3−7 behaves differently with changing t_{inj}. For Cases 3−4, the direct injection of octane is supplied prior to the onset of the LTHR. The overall combustion of Cases 3−4 is retarded with advancing t_{inj}. The retarded combustion phasing of Cases 3−4 is attributed to the noticeable drop in pressure and temperature caused by the octane evaporation (Fig. 7a). The drop in pressure and temperature also affect the LTHR of Case 3, delaying

the first-stage ignition of Case 3, which in turn retards the main combustion (Fig. 7c).

For Cases 5−7, the remaining octane is delivered after the end of the LTHR. Similar to Case 3, the overall combustion of Case 5 is also delayed due to T_{drop} caused by the octane injection. However, T_{drop} affects the intermediate-temperature heat release (ITHR) of Case 5 rather than the LTHR as in Case 3. For Case 5 octane is delivered at t_{inj} = -5.5°CA ATDC at which the temperature range of 930−946K (not shown here) is intermediate temperature. In general, the temperature drop increases the induction time of the second-stage ignition. This is mainly because the hydrogen peroxide (H_2O_2) decomposition via the chain-branching reaction ($H_2O_2 + M \rightarrow OH + OH + M$) becomes active above, say, 1000 K. Therefore, the small drop of temperature prohibits the occurrence of this reaction, consequently delaying the start of the second-stage ignition [15, 16]. The ITHR reactions are typically a relatively slow process compared to those of the HTHR. As a result, the decomposition and consumption of *iso*-octane take a longer time compared to Cases 6−7 such that Case 5 has the retarded combustion phasing to Case 6−7.

On the contrary, the combustion characteristic of Cases 6 and 7 proceeds differently in two stages. For both Cases 6 and 7, prior to the remaining octane introduced, the fuel/air has undergone the HTHR as a typical RCCI combustion mode−so-called the

combustion stage-I. The combustion stage-I determines the start of the main combustion with a moderate HRR relative to that of RCCI (Case 2). The remaining octane is then introduced into the burning charge, and hence, it burns quickly (see Fig. 8b). The starting point of the remaining octane induction initiates the second stage of combustion, so-call the combustion stage-II. During the combustion stage-II, the injection rate of iso-C_8H_{18} directly controls the consumption rate of iso-C_8H_{18}, which in turn governs the rate and peak of heat release of the combustion stage-II. As can be seen in Fig. 8b, iso-C_8H_{18} starts injecting at $t_{inj} = 2.3$ °CA ATDC at which the corresponding mean temperature is approximately 1200 K, and main combustion is already in progress. Under such high T, the introduced iso-C_8H_{18} burns immediately, and hence, the consumption of iso-C_8H_{18} coincides with the production of heat.
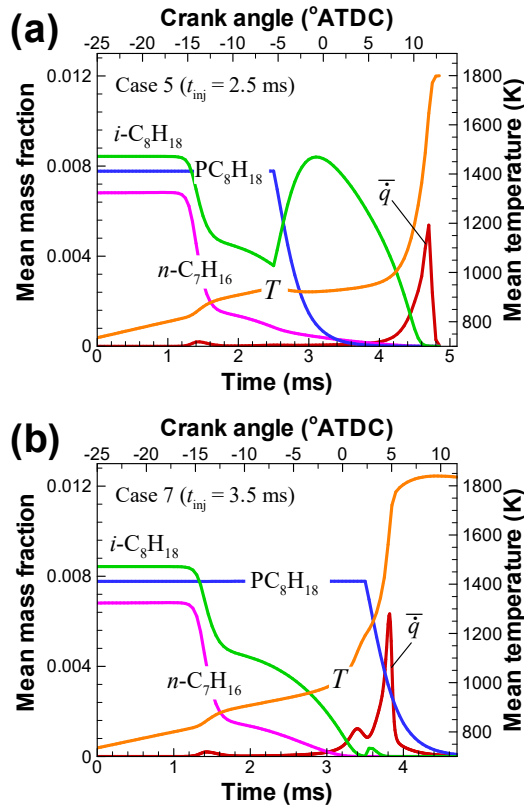

Figure 8. Temporal evolutions of the mean mass fraction of octane, PC_8H_{18}, and heptane, temperature, and HRR for Cases 5 & 7.

These findings are consistent with those by Wissink and Reitz [3-5]. They demonstrated that DDFS combustion is the mixing-controlled burn of the last direct injection DDFS, so-called 'diffusion-limited injection'. The timing and duration of the diffusion-limited injection allow precise control over the rate of heat release and pressure rise. However, the t_{inj} range was limited after the end of the LTHR and also constrained by a trade-off between NOx and soot.

4. Conclusion

Direct dual fuel stratification (DDFS) and reactivity controlled compression ignition (RCCI) combustion were performed using 2-D direct numerical simulations (DNSs). By varying the injection timing, t_{inj}, the effect of t_{inj} on the ignition characteristics of primary reference fuel (PRF)/air mixtures under DDFS conditions are numerically investigated with a 116-species reduced mechanism of PRF oxidation. In the DDFS combustion, a premixed background charge is prepared through an early injection of a main portion of gasoline, then followed by direct injections of diesel and the remaining gasoline. The remaining gasoline is supplied near the top dead center (TDC) at the time when the low-temperature heat release (LTHR) already completed. A pseudo iso-C_8H_{18} model is developed to account for the late injection event. n-Heptane and iso-octane are chosen as two fuels of low and high reactivity, respectively. The corresponding global PRF number is PRF70. The effects of compression heating and expansion cooling by the piston motion of in an engine cylinder are also taken into account by adopting a compression heating/cooling model.

It is found that DDFS combustion is highly sensitive to the injection timing, t_{inj}. The combustion phasing tends to be delayed with the late iso-octane injection near TDC. When iso-octane is delivered just near the TDC into the undergoing-combustion charge, the overall combustion from this point occurs dominantly through autoignition. Its burn rate is primarily governed by diffusion-limited injection. As a result, the HRR is still well-controlled and entirely dependent on the timing and duration of late iso-octane injection. Compared to DDFS combustion, it is also found that RCCI combustion shows a higher peak heat release rate due to a shorter combustion duration compared to DDFS cases.

In summary, DDFS combustion concept with stratification in both iso-octane and n-heptane offers a great potential in extending the upper load limit of RCCI combustion by allowing the more flexible capability of manipulating its combustion process with the help of optimum injection strategies.

References

[1] R.D. Reitz, G. Duraisamy, Prog. Energy Combust. Sci. 46 (2015) 12–71.
[2] R.D. Reitz, G. Duraisamy, Prog. Energy Combust. Sci. 46 (2015) 12–71.
[3] M. Wissink, R.D. Reitz, SAE Int. J. Engines 8 (2015) 878–889.

[4] M. Wissink, R. Reitz, Int. J. Engine (2016) 1468087416661867.

[5] M. Wissink, R. Reitz, SAE Int. J. Engines 9 (2016) 1036–1048.

[6] C.S. Yoo, T. Lu, J.H. Chen, C.K. Law, Combust. Flame 158 (2011) 1727–1741.

[7] C.S. Yoo, Z. Luo, T. Lu, H. Kim, J.H. Chen, Proc.Combust. Inst. 34 (2013) 2985

[8] M.B. Luong, Z. Luo, T. Lu, S.H. Chung, C.S. Yoo, Combust. Flame 160 (2013) 2038–2047.

[9] M.B. Luong, T. Lu, S.H. Chung, C.S. Yoo, Combust. Flame 161 (2014) 2878–2889.

[10] S.O. Kim, M.B. Luong, J.H. Chen, C.S. Yoo, Combust. Flame 162 (2015) 717–726.

[11] M.B. Luong, G.H. Yu, T. Lu, S.H. Chung, C.S. Yoo, Combust. Flame 162 (2015) 4566–4585.

[12] M.B. Luong, G.H. Yu, S.H. Chung, C.S. Yoo, Proc. Combust. Inst., in press, (2016), http://dx.doi.org/10.1016/j.proci.2016.08.038

[13] M.B. Luong, G.H. Yu, S.H. Chung, C.S. Yoo, Proc. Combust. Inst., in press, (2016), http://dx.doi.org/10.1016/j.proci.2016.06.076

[14] A. Bhagatwala, R. Sankaran, S. Kokjohn, J.H. Chen, Combust. Flame 162 (2015) 3412–3426.

[15] C. K. Westbrook, Proc. Combust. Inst. 28 (2000) 1563–1577.

[16] W. Hwang, J. Dec, M. Sjöberg, Combust. Flame 154 (2008) 387–409.